

## Interplay of Magnetism and Topological Superconductivity in Bilayer Kagome Metals

Santu Baidya,<sup>1,\*</sup> Aabhaas Vineet Mallik<sup>2,†</sup>, Subhro Bhattacharjee,<sup>2,‡</sup> and Tanusri Saha-Dasgupta<sup>3,§</sup>

<sup>1</sup>*Department of Physics and Astronomy, Rutgers, The State University of New Jersey, Piscataway, New Jersey 08854-8019, USA*

<sup>2</sup>*International Centre for Theoretical Sciences, Tata Institute of Fundamental Research, Bengaluru 560 089, India*

<sup>3</sup>*Department of Condensed Matter Physics and Materials Science, S. N. Bose National Centre for Basic Sciences, Kolkata 700098, India*



(Received 23 February 2020; accepted 15 June 2020; published 8 July 2020)

The binary intermetallic materials,  $M_3\text{Sn}_2$  ( $M = 3d$  transition metal) present a new class of strongly correlated systems that naturally allows for the interplay of magnetism and metallicity. Using first principles calculations we confirm that bulk  $\text{Fe}_3\text{Sn}_2$  is a ferromagnetic metal, and show that  $M = \text{Ni}$  and  $\text{Cu}$  are paramagnetic metals with nontrivial band structures. Focusing on  $\text{Fe}_3\text{Sn}_2$  to understand the effect of enhanced correlations in an experimentally relevant atomistically thin single kagome bilayer, our *ab initio* results show that dimensional confinement naturally exposes the flatness of band structure associated with the bilayer kagome geometry in a resultant ferromagnetic Chern metal. We use a multistage minimal modeling of the magnetic bands progressively closer to the Fermi energy. This effectively captures the physics of the Chern metal with a nonzero anomalous Hall response over a material relevant parameter regime along with a possible superconducting instability of the spin-polarized band resulting in a topological superconductor.

DOI: [10.1103/PhysRevLett.125.026401](https://doi.org/10.1103/PhysRevLett.125.026401)

**Introduction.**—Accentuated quantum fluctuations due to dimensional confinement and electron-electron correlations are at the heart of some of the novel electronic phases of condensed matter—e.g., high temperature superconductivity in cuprates [1] and iron pnictides [2]; the low-dimensional frustrated magnets [3]; easily exfoliable materials such as monolayer and bilayer graphene [4,5]; and two-dimensional (2D) electron gas leading to integer and fractional quantum Hall effects [6] in synthetic heterostructures [7,8].

A recent addition to this ongoing research is the binary intermetallic series  $M_mX_n$  with  $M = 3d$  transition metals (TMs) forming stacked kagome layers, separated by  $X = \text{Sn}, \text{Ge}$  spacer layers in stoichiometric ratios of  $m:n = 3:1, 3:2,$  or  $1:1$ . Recent experiments report the observation of bulk Dirac cones in the electron band structure [9,10], large anomalous Hall response [11–14] as well as magnetic Weyl excitations [15] in them. Diverging density of states, probed by scanning tunneling spectroscopy, have been reported for  $\text{Fe}_3\text{Sn}_2$  [16] as well as for the ternary kagome ferromagnetic compound,  $\text{Co}_3\text{Sn}_2\text{S}_2$  [17], though the existence of flatband, a characteristic of kagome geometry, has remained inconclusive possibly due to hybridization with other bands in the 3D material. Recently synthesized, [18] bulk  $\text{FeSn}$  has been claimed to have flatbands at energies few hundreds of meV below and above Fermi level. In this backdrop, it is curious to explore the consequence of dimensional confinement in these intermetallics by considering the atomistically thin limit of these

materials which is expected to further enhance the strong correlation physics and thereby providing a platform for the interplay of flatband physics and fluctuating magnetism in the low-dimensional itinerant systems containing  $3d$  TMs.

In this Letter, we explore the above possibility within the framework of *ab initio* density functional theory (DFT) and effective low-energy minimal models inspired by the DFT band structure. To probe the effect of dimensional confinement, we consider one unit of kagome bilayer derived from the bulk structure [Fig. 1(a)], sandwiched between two Sn layers [Fig. 1(b)]. Also, in addition to Fe compound which is already synthesized as a bulk material, we consider two more late TM based compounds—Ni and Cu—which are yet to be synthesized, in order to understand the generic behavior of this family of materials. The calculated cleavage energy [19,20] costs involved in the creation of a bilayer is  $1\text{--}2 \text{ J/m}^2$  [21]—similar to that required for creating 2D MXenes, the 2D counterparts of MAX phases [25,26], which have already been successfully synthesized through chemical etching.

Analysis of the electronic structure of bulk  $M_3\text{Sn}_2$  ( $M = \text{Fe}, \text{Ni},$  and  $\text{Cu}$ ) prompts us to conclude that  $\text{Fe}_3\text{Sn}_2$  is the natural choice to search for fluctuation driven physics in magnetic flatbands, as both  $\text{Ni}_3\text{Sn}_2$  and  $\text{Cu}_3\text{Sn}_2$  turn out to be nonmagnetic within our DFT calculations. Thus, while  $\text{Ni}_3\text{Sn}_2$  and  $\text{Cu}_3\text{Sn}_2$  have interesting band structures (see below) and hence deserve attention, Fe appears to be in a sweet spot of the interplay of correlations

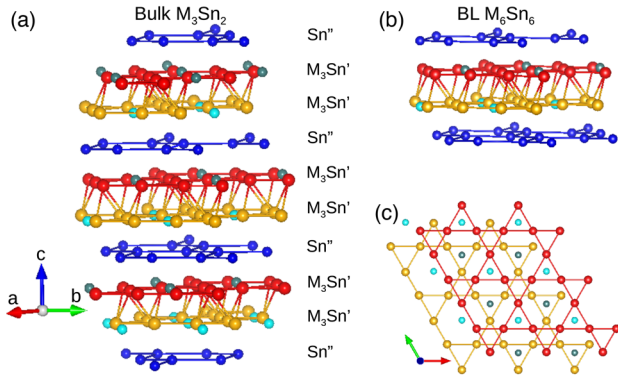


FIG. 1. (a) Layered arrangement in bulk  $M_3\text{Sn}_2$ . (b) Bilayer  $M_6\text{Sn}_6$  derived out of the bulk layered structure. (c) Stacking of two kagome layers within the bilayer, viewed along the out-of-plane direction.

and band physics in the late  $3d$  TM series. Our DFT calculations for bilayer  $\text{Fe}_3\text{Sn}_2$  reveal that confinement to the bilayer limit results in the formation of near flatbands within  $\pm 10$  meV of the Fermi level, together with massive Weyl-like band features. Interestingly, the ferromagnetic correlations in the 3D compound are found to survive down to bilayer limit. The resulting almost flatbands have non-zero Chern number, realizing a Chern metal in the bilayer system. Inclusion of magnetic fluctuation effects within the model calculations of the kagome bilayer lead to a fluctuation-driven topological superconductor.

**Electronic structure of bulk  $M_3\text{Sn}_2$ .**—Rhombohedrally structured bulk  $M_3\text{Sn}_2$  consists of kagome bilayers of  $M$  atoms sandwiched between stanene layers ( $\text{Sn}''$  atoms) as shown in Fig. 1(a) [27]. The crystal structure [21] allows for a breathing anisotropy in each kagome plane resulting in unequal sizes of the up and down triangles in the kagome planes [Fig. 1(c)]. The crystal structures of  $\text{Ni}_3\text{Sn}_2$  and  $\text{Cu}_3\text{Sn}_2$  are obtained from that of  $\text{Fe}_3\text{Sn}_2$  through symmetry-allowed relaxation.

The DFT calculations were performed in plane wave basis using the Vienna Ab initio Simulation Package [28,29] with exchange-correlation functional within generalized gradient approximation (GGA) [30]. Also, the correlation effect at TM sites is included within GGA +  $U$  [31] with  $U = 0.5$  eV [32]. Weak spin-orbit coupling (SOC) is also included for the TM  $3d$  states which appears to be a crucial ingredient to drive the topological behavior as well as the stability of magnetism in the bilayer limit (see below). Further details are provided in the Supplemental Material (SM) [21]. Figures 2(a)–2(c) show the GGA +  $U$  + SOC band structure of  $\text{Fe}_3\text{Sn}_2$ ,  $\text{Ni}_3\text{Sn}_2$ , and  $\text{Cu}_3\text{Sn}_2$  plotted along the high symmetry directions of the hexagonal Brillouin zone (BZ) [33].

Interestingly, while the DFT calculations for  $\text{Fe}_3\text{Sn}_2$  stabilize a ferromagnet at the Fe sites with moment  $\approx 2.2\mu_B$ , in agreement with reported experiments [32], both Ni and Cu compounds turned out to be paramagnetic. Focusing on

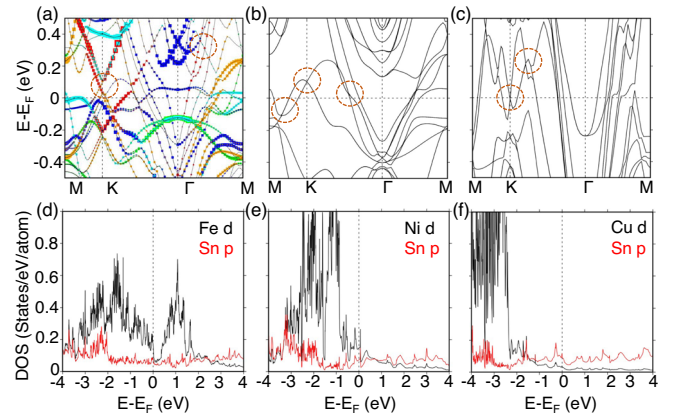


FIG. 2. GGA +  $U$  + SOC band structure of bulk ferromagnetic  $\text{Fe}_3\text{Sn}_2$  (a), paramagnetic  $\text{Ni}_3\text{Sn}_2$  (b), and  $\text{Cu}_3\text{Sn}_2$  (c). The nontrivial Weyl and Dirac-like crossings are circled. In (a) the Fe  $d$  orbital character is shown—red,  $d_{xy}$ ; green,  $d_{yz}$ ; cyan,  $d_{xz}$ ; blue,  $d_{3z^2-r^2}$ ; yellow,  $d_{x^2-y^2}$ . The corresponding non-spin-polarized projected DOS are shown for the Fe (d), Ni (e), and Cu (f) compounds.

the corresponding density of states (DOS) [Figs. 2(d)–2(f)], we find that while in case of  $\text{Fe}_3\text{Sn}_2$ , the low-energy states are primarily dominated by Fe  $d$  states with a small admixture from Sn  $p$  due the covalency, for  $\text{Ni}_3\text{Sn}_2$  and  $\text{Cu}_3\text{Sn}_2$  there is a progressively higher contribution of the Sn  $p$  orbitals such that for Cu it is almost entirely of Sn  $p$  character. The Stoner criteria of magnetism, appropriate for metallic systems, gives  $I \times N(E_F)$  [ $I$  = Stoner parameter,  $N(E_F) = \text{DOS at } E_F$ ] to be larger than one (1.4) for  $\text{Fe}_3\text{Sn}_2$ , and significantly less than 1 for  $\text{Ni}_3\text{Sn}_2$  and  $\text{Cu}_3\text{Sn}_2$  (0.3 and 0.1, respectively), justifying the ferromagnetic (paramagnetic) ground state in the Fe (Ni and Cu) system(s). The band structures of  $\text{Fe}_3\text{Sn}_2$ , which is in good agreement with literature [32], and that of  $\text{Ni}_3\text{Sn}_2$  and  $\text{Cu}_3\text{Sn}_2$  show topologically nontrivial Weyl and Dirac points [Figs. 2(a)–2(c)]. The electronic structure of  $\text{Ni}_3\text{Sn}_2$  and  $\text{Cu}_3\text{Sn}_2$  compounds though appears interesting and deserves further attention, in keeping the focus on the interplay of magnetic fluctuations, topological properties, and low dimensionality, we discuss the properties of bilayers of  $\text{Fe}_3\text{Sn}_2$  in the rest of this Letter.

**Electronic structure of bilayer  $\text{FeSn}$ .**—The  $\text{Sn}''$  terminated  $\text{Fe}_6\text{Sn}_6$  bilayer is shown in Fig. 1(b). The kagome bilayer, which in this case is isolated, consists of two kagome layers of Fe atoms, shifted with respect to each other. It is important to note that the bulk  $\text{FeSn}$  structure studied recently [18] consists of alternate Fe-kagome layers and Sn layers and hence is different from the present case.

The GGA + SOC +  $U$  band structure of the Sn-terminated bilayer  $\text{FeSn}$  [cf. Fig. 1(b)] is shown in Fig. 3 along with the orbital characters of the bands projected to the Fe  $d$ . DFT estimate for intra- and interkagome layer magnetic interactions for the above bilayer are both ferromagnetic—as in bulk  $\text{Fe}_3\text{Sn}_2$ —with magnitudes  $\approx 10$  meV and

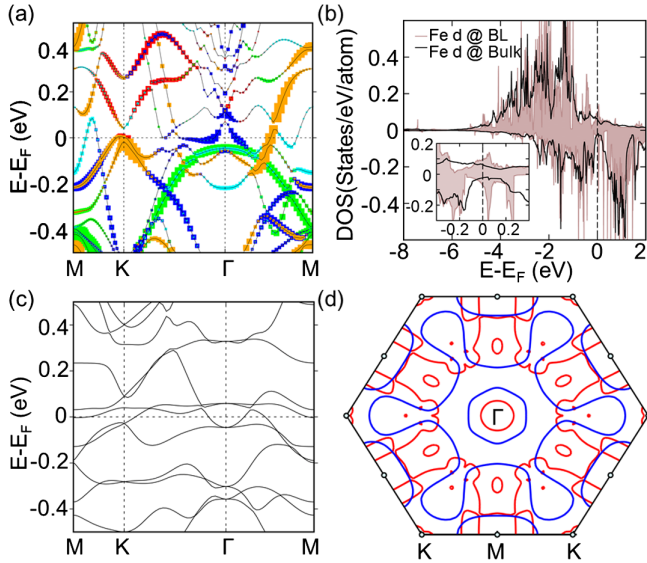


FIG. 3. GGA + SOC +  $U$  band structure (a) and Fe  $d$  projected spin-polarized DOS, with positive (negative) axis corresponding to DOS in up (down) spin channel (b) of bilayer Fe compound in the FM state. In (a) the Fe  $d$  orbital characters are denoted with different colors—red,  $d_{xy}$ ; green,  $d_{yz}$ ; cyan,  $d_{xz}$ ; blue,  $d_{3z^2-r^2}$ ; and yellow,  $d_{x^2-y^2}$ . (b) Shows a comparison between the bilayer and bulk DOS, while the inset shows the van Hove features of the two-dimensional electronic structure of the bilayer. (c) Band structure of bilayer in nonmagnetic state. (d) The Fermi surface in the nonmagnetic (blue) and ferromagnetic states (red).

$\approx 0.3$  meV, respectively. This is in contrast to magnetic behavior of bulk FeSn reported recently [18], where the ferromagnetic Fe kagome layers are coupled antiferromagnetically.

The bilayer band structure shown in Fig. 3(a) should be contrasted with the bulk electronic band structure [Fig. 2(a)]. The latter is characterized by several low-energy bands having non-Fe character as expected for a three-dimensional network of the Sn atoms in the bulk. In comparison, the band structure of bilayer FeSn within  $\pm 10$  meV is primarily of Fe  $d_{x^2-y^2}$ ,  $d_{xy}$  and  $d_{3z^2-r^2}$  characters, with little contribution from Sn  $p$ . While the basic features of the bilayer DOS, presented in Fig. 3(b), is similar to that of bulk, close observation reveals [inset of Fig. 3(b)] formation of van Hove-like singularities in the DOS of the bilayer arising from dimensional confinement. This is further confirmed by calculating effective masses of the low-energy bands. While the parallel components of effective masses range between  $3-5m_e$ , that in perpendicular direction is  $1000-2000m_e$ .

Most importantly, in contrast to the bulk band structure, the bilayer band structure shows a couple of somewhat *flatbands*, arising due to destructive interference of hoppings in the kagome bilayers, in an energy window of  $\pm 10$  meV around the Fermi level  $E_F$  in a forced paramagnetic state [Fig. 3(c)]. They survive, albeit somewhat dispersive, in the magnetic state [Fig. 3(a)]. The Fermi

surface of the paramagnetic and ferromagnetic states are shown in Fig. 3(d). The reconstruction of the Fermi surface due to ferromagnetic order resulting in small electron- and holelike pockets is apparent.

The nearly flatbands span a significant portion of the BZ and should be contrasted with the case of bulk FeSn structure [18] consisting of kagome monolayers, where the flatband features occur at few hundred meV from  $E_F$ . Because of ferromagnetic order, time-reversal symmetry is broken and these flatish bands acquire a finite Chern number. Constructing the maximally localized Wannier functions using WANNIER90 [34], we calculated the integrated Berry curvature over the 2D BZ. This gives a Chern number of  $-1$  for the flatband closest to  $E_F$ . Thus, the DFT results show that bilayer FeSn may stabilize a ferromagnetic Chern metal [35,36] with nonquantized but large anomalous Hall response.

*Effective tight-binding model.*—Based on our DFT findings, we conclude that geometric confinement to bilayer results in (a) quasi-2D electronic structure, (b) survival of ferromagnetic correlation, and (c) realization of almost flatbands. The effect of fluctuations on almost flatbands is expected to be strong, opening up possibilities for stabilizing novel phases. The intricate features of the low-energy DFT bands near  $E_F$  [cf. Fig. 3(a)] require a detailed tight-binding model accounting for the various hopping processes involved. Here instead, we construct simpler tight-binding models with the right orbital character and short-range hopping that capture qualitatively the low-energy DFT band structure and use them to study the effect of correlation and band properties.

To this end we introduce two related symmetry-allowed models, (1) a three orbital (plus spin)–site model in which we account for the magnetization within mean field decomposition of on site Hubbard interactions in the ferromagnetic channel. This captures the large anomalous Hall response in the Chern metal phase [Fig. 4(b)] in a material relevant parameter regime; and (2) an even more simplified one spin-polarized orbital–site tight-binding model which captures the flatish band near the Fermi level which we use to study the possible superconductivity driven by magnetic fluctuations within a self consistent Bardeen-Cooper-Schrieffer (BCS) mean field theory. We expect that since the superconductivity arises from the instability of the Fermi surface the minimal one orbital model gives a valid qualitative description of such phases. The parameters of both the models reveal that while the nearest neighbor hopping within each kagome layer dominates [21], further neighbor and interlayer hoppings are non-negligible—indicating differences in the nature of the almost flatbands in bilayers from that in a single-layer kagome.

Our minimal tight-binding modeling starts by [21,37] including three Fe  $d$  orbitals per site— $d_{3z^2-r^2}$ ,  $d_{x^2-y^2}$ , and  $d_{xy}$ —which contribute to the electronic states within  $\pm 10$  meV of the DFT band structure [cf. Fig. 3(a)]. This

generic symmetry-allowed model allows intra- and inter-kagome layer first, second, and third nearest neighbor hopping among the orbitals, along with (weak) SOC projected to the above orbitals. As noted above, the breathing anisotropy within each kagome layer generically leads to a difference in the hopping amplitude on bigger triangles compared to smaller triangles. We introduce a parameter  $r$  in the tight-binding model as the ratio of the nearest neighbor hopping amplitudes on bigger triangles to that on smaller triangles. Generically, we do not know the value of  $r$  in bilayer FeSn and related materials. Further, it is possible that the actual value may depend on synthesis process and substrate and therefore is an experimentally relevant parameter which we vary to study various properties. Tuning the parameters of this model [21] lead to a representative tight-binding band structure in Fig. 4(a) with  $r = 1.25$  which is in semiquantitative agreement with the DFT results [Fig. 3(a)].

*Chern metal and anomalous Hall effect.*—As suggested by our WANNIER90 Chern number calculation mentioned above, the bands close to the Fermi level in Fig. 4(a) also have nonzero Chern numbers. While it is complicated to calculate the Chern numbers of the individual bands since they cross, a more robust quantity is the anomalous Hall response of the resultant Chern metal. We plot the anomalous Hall conductivity ( $\sigma_{xy}$ ) as a function of the asymmetry parameter  $r$  in Fig. 4(b) where other band parameters are

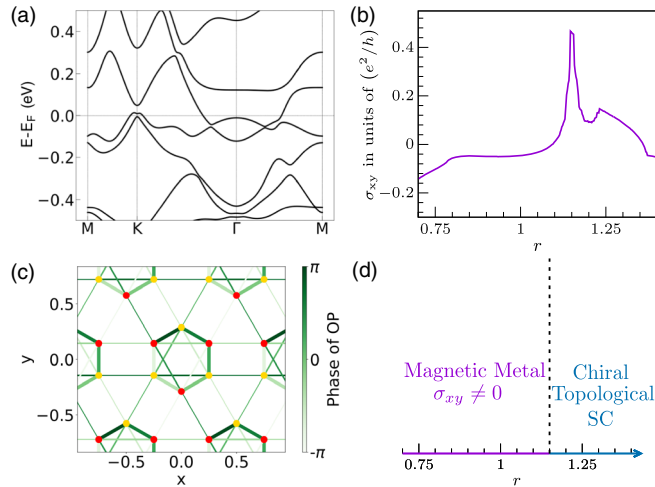


FIG. 4. Panel (a) shows tight-binding bands obtained for a three orbital model with parameters tuned to reproduce qualitative agreement with the DFT results. Panel (b) shows the evolution of  $\sigma_{xy}$  as a function of the breathing anisotropy parameter  $r$  (see text). Panel (c) shows the superconducting order parameter in the reduced one orbital spin-polarized tight-binding model with nearest neighbor attractive interactions mediated by ferromagnetic fluctuations. The thickness of the bonds is proportional to the amplitude of the superconducting order parameter and the colors encode its phase. Panel (d) shows the topological superconductor and magnetic metal (with  $\sigma_{xy} \neq 0$ ) as a function of  $r$  for the one-orbital tight-binding model.

kept fixed. The resultant finite response over a wide parameter regime  $r \in (0.7 - 1.4)$  indicates that the anomalous Hall response is a robust feature of Chern metal in bilayer FeSn and allied materials.

The Chern metal is an extremely interesting phase where the partially filled band has a topological invariant. The instability of such a metallic phase therefore involves an intricate interplay of band topology and correlations. In the presence of small SOC, we expect the ferromagnetic order to be stable at finite temperatures even in the bilayer, albeit with enhanced magnetic fluctuations. These magnetic fluctuations can then act as a pairing glue leading to superconductivity in the spin-polarized band. We now focus on the possibility of realizing such a magnetic fluctuation driven superconductor.

*Superconductivity.*—Both the DFT and the tight-binding model show the presence of small Fermi pockets near the  $K$  and the  $\Gamma$  points of the BZ arising from the almost flat low-energy bands [Figs. 3(d) and 4(a)]. Magnetic fluctuations lead to effective attractive interactions for electrons—driving a superconducting instability naturally in the triplet channel for the spin-polarized bands [38–42]. This superconductivity can be explored within a self-consistent BCS mean field theory. For this purpose we use a symmetry-allowed effective tight-binding model with one spin-polarized orbital–site of the kagome bilayer, with parameters chosen such that the DFT bands close to  $E_F$  are well represented [21]. Further, integrating out the magnetic fluctuations leads to short-range (nearest neighbor in our case) attractive interactions  $V$  between the electronic densities,  $\sim -V \sum_{\langle ij \rangle} n_i n_j$ . Within a multiband BCS mean field theory, the above model indeed stabilizes a superconductor for a wide regime of the parameter  $r$  when  $V \sim t$  [21], where  $t$  is the nearest neighbor hopping of the effective low-energy one-orbital tight-binding model. The fairly large value of the interaction can be attributed to the small density of states at  $E_F$  due to the small Fermi pockets. Here, we plot the results for the representative choice of  $V = 2t$ . A rough estimate of effective low-energy scales gives  $t \sim 0.13$  eV and hence  $V \sim 0.26$  eV  $\approx 0.5U$  [21].

In our analysis, we incorporate eighteen pairing order parameters corresponding to the nearest neighbor bonds associated with a unit cell [21]. In Fig. 4(c) we show the superconducting order with the thickness of a bond being proportional to its magnitude and the color of the bond encoding its phase. The maximum pairing amplitude is  $\sim 0.02t$  which would correspond to a mean field transition temperature of  $\sim 10$  K. A straightforward analysis reveals that the pairing amplitudes in Fig. 4(c) transform like a  $l_z = 1$  orbital under a rotation by  $2\pi/3$  about the center of the hexagon of the bilayer akin to  $p_x + ip_y$  superconductor [39]. The topological nature of superconductivity in this system is easily confirmed by computing the net Chern number of the negative energy Bogoliubov bands [43–46].

Remarkably, this topological superconductor is stable over a wide range of the breathing anisotropy parameter  $r$ , which is promising in regard to its experimental detection. For sufficiently small values of  $r$  superconductivity ceases to exist and one recovers a magnetic metal exhibiting anomalous Hall response. This is shown in Fig. 4(d).

*Summary and outlook.*—Our DFT results show that kagome intermetallic series derived from bulk  $M_3\text{Sn}_2$  ( $M = \text{Fe}, \text{Ni}, \text{Cu}$ ) can host a rich interplay of band physics and correlations. To the best of our knowledge, while only bulk  $\text{Fe}_3\text{Sn}_2$  has been synthesized, the Ni and Cu counterparts provide future avenues to explore. The above interplay is most prominent in the case of Fe where dimensional confinement in the bilayer limit enhances it by stabilizing a ferromagnetic metal with nearly flatbands near the Fermi level and thereby giving a Chern metal with large anomalous Hall conductivity. Instability of this Chern metal, within a low-energy tight-binding model and BCS mean field theory results in a topological superconductor in a material relevant parameter regime. A related instability, particularly relevant for the nearly flatband Chern metal, is a magnetic fluctuation driven fractional Chern insulator. It would be interesting to investigate the relevance of such a novel phase in the present context. All the above ingredients have close similarity with the rich physics of twisted bilayer graphene and hence experimental progress in isolating bilayer  $\text{Fe}_3\text{Sn}_2$  and related materials may open up newer playgrounds of novel correlated physics probing the interplay of band topology, electron-electron correlations, and spontaneous symmetry breaking.

The authors thank H. R. Krishnamurthy, V. B. Shenoy, S. Nakatsuji, J. Checkelsky, M. Jain, and A. Agarwala for useful discussions. The authors thank Yogesh Singh for a careful reading of the manuscript. T. S. D. and S. Bh. thank Jawaharlal Nehru University, New Delhi; ICTS-TIFR, Bangalore; and S. Bh. thanks ISSP, Tokyo for hospitality during different stages of this project. A. V. M. and S. Bh. acknowledge financial support through Max Planck partner group on strongly correlated systems at International Centre for Theoretical Sciences; SERB-DST (government of India) early career research grant (No. ECR/2017/000504) and the Department of Atomic Energy, government of India, under Project No. 12-R&D-TFR-5.10-1100.

S. B. and A. V. M. have contributed equally to this work.

\*santubaidya2009@gmail.com

†aabhaas.iiser@gmail.com

‡subhro@icts.res.in

§t.sahadasgupta@gmail.com

- [1] A. Damascelli, Z. Hussain, and Z.-X. Shen, *Rev. Mod. Phys.* **75**, 473 (2003).  
 [2] Q. Si, R. Yu, and E. Abrahams, *Nat. Rev. Mater.* **1**, 16017 (2016).

- [3] O. A. Starykh, *Rep. Prog. Phys.* **78**, 052502 (2015).  
 [4] M. J. Allen, V. C. Tung, and R. B. Kaner, *Chem. Rev.* **110**, 132 (2010).  
 [5] A. H. MacDonald, *Physics* **12**, 12 (2019).  
 [6] A. Tsukazaki, A. Ohtomo, T. Kita, Y. Ohno, H. Ohno, and M. Kawasaki, *Science* **315**, 1388 (2007).  
 [7] A. Ohtomo and H. Y. Hwang, *Nature (London)* **427**, 423 (2004).  
 [8] M. Zhang, K. Du, T. Ren, H. Tian, Z. Zhang, H. Y. Hwang, and Y. Xie, *Nat. Commun.* **10**, 4026 (2019).  
 [9] L. Ye, M. Kang, J. Liu, F. von Cube, C. R. Wicker, T. Suzuki *et al.*, *Nature (London)* **555**, 638 (2018).  
 [10] G. L. Caer, B. Malaman, and B. Roques, *J. Phys. F* **8**, 323 (1978).  
 [11] S. Nakatsuji, N. Kiyohara, and T. Higo, *Nature (London)* **527**, 212 (2015).  
 [12] N. Kiyohara, T. Tomita, and S. Nakatsuji, *Phys. Rev. Applied* **5**, 064009 (2016).  
 [13] A. K. Nayak, J. E. Fischer, Y. Sun, B. Yan, J. Karel, A. C. Komarek *et al.*, *Sci. Adv.* **2**, e1501870 (2016).  
 [14] J. Yan, X. Luo, H. Y. Lv, Y. Sun, P. Tong, W. J. Lu, X. B. Zhu, W. H. Song, and Y. P. Sun, *Appl. Phys. Lett.* **115**, 102404 (2019).  
 [15] K. Kuroda, T. Tomita, M.-T. Suzuki, C. Bareille, A. A. Nugroho, P. Goswami *et al.*, *Nat. Mater.* **16**, 1090 (2017).  
 [16] Z. Lin, J. H. Choi, Q. Zhang, W. Qin, S. Yi, P. Wang *et al.*, *Phys. Rev. Lett.* **121**, 096401 (2018).  
 [17] J.-X. Yin, S. S. Zhang, G. Chang, Q. Wang, S. S. Tsirkin, Z. Guguchia *et al.*, *Nat. Phys.* **15**, 443 (2019).  
 [18] M. Kang, L. Ye, S. Fang, J.-S. You, A. Levitan, M. Han *et al.*, *Nat. Mater.* **19**, 163 (2020).  
 [19] R. Benedek and M. M. Thackeray, *Phys. Rev. B* **83**, 195439 (2011).  
 [20] D. Santos-Carballal, A. Roldan, R. Grau-Crespo, and N. H. de Leeuw, *Phys. Chem. Chem. Phys.* **16**, 21082 (2014).  
 [21] See Supplemental Material at <http://link.aps.org/supplemental/10.1103/PhysRevLett.125.026401>, which provides further discussion on the following topics: (i) DFT computations including cleavage energy, and relaxed crystal structure; (ii) analysis using model tight-binding Hamiltonians including the computation of Hall conductivity, possible superconducting instability, and its topological nature. It includes Refs. [22–24].  
 [22] G. Kresse and J. Furthmüller, *Comput. Mater. Sci.* **6**, 15 (1996).  
 [23] H.-M. Guo and M. Franz, *Phys. Rev. B* **80**, 113102 (2009); K. Sun, Z. Gu, H. Katsura, and S. Das Sarma, *Phys. Rev. Lett.* **106**, 236803 (2011).  
 [24] T. A. Maier, A. Macridin, M. Jarrell, and D. J. Scalapino, *Phys. Rev. B* **76**, 144516 (2007); T. Dahm, V. Hinkov, S. V. Borisenko, A. A. Kordyuk, V. B. Zabolotnyy, J. Fink, B. Büchner, D. J. Scalapino, W. Hanke, and B. Keimer, *Nat. Phys.* **5**, 217 (2009).  
 [25] K. Mondal and P. Ghosh, *Solid State Commun.* **299**, 113657 (2019).  
 [26] M. Naguib, V. N. Mochalin, M. W. Barsoum, and Y. Gogotsi, *Adv. Mater.* **26**, 992 (2013).  
 [27] H. Giefers and M. Nicol, *J. Alloys Compd.* **422**, 132 (2006).  
 [28] G. Kresse and D. Joubert, *Phys. Rev. B* **59**, 1758 (1999).

- [29] G. Kresse and J. Furthmüller, *Phys. Rev. B* **54**, 11169 (1996).
- [30] J. P. Perdew, K. Burke, and M. Ernzerhof, *Phys. Rev. Lett.* **77**, 3865 (1996).
- [31] V. I. Anisimov, F. Aryasetiawan, and A. I. Lichtenstein, *J. Phys. Condens. Matter* **9**, 767 (1997).
- [32] M. Yao, H. Lee, N. Xu, Y. Wang, J. Ma, O. V. Yazyev *et al.*, [arXiv:1810.01514](https://arxiv.org/abs/1810.01514).
- [33] The SOC calculations for  $\text{Fe}_3\text{Sn}_2$  were carried out considering the magnetization axis pointed along  $x$  ( $M_x$ ),  $y$  ( $M_y$ ), or  $z$  ( $M_z$ ) directions, which showed the energy corresponding to  $M_z$  to be lower compared to  $M_x$  or  $M_y$ . The results are thus shown for only the  $M_z$  direction.
- [34] A. A. Mostofi, J. R. Yates, Y.-S. Lee, I. Souza, D. Vanderbilt, and N. Marzari, *Comput. Phys. Commun.* **178**, 685 (2008).
- [35] A. Mishra and S. B. Lee, *Sci. Rep.* **8**, 799 (2018).
- [36] C. Hickey, P. Rath, and A. Paramekanti, *Phys. Rev. B* **91**, 134414 (2015).
- [37] G. Xu, B. Lian, and S.-C. Zhang, *Phys. Rev. Lett.* **115**, 186802 (2015).
- [38] B. Wu, G. Bastien, M. Taupin, C. Paulsen, L. Howald, D. Aoki, and J.-P. Brison, *Nat. Commun.* **8**, 14480 (2017).
- [39] W.-S. Wang, Y.-C. Liu, Y.-Y. Xiang, and Q.-H. Wang, *Phys. Rev. B* **94**, 014508 (2016).
- [40] N. F. Berk and J. R. Schrieffer, *Phys. Rev. Lett.* **17**, 433 (1966).
- [41] S. Doniach and S. Engelsberg, *Phys. Rev. Lett.* **17**, 750 (1966).
- [42] K. V. Samokhin and V. P. Mineev, *Phys. Rev. B* **77**, 104520 (2008).
- [43] X.-L. Qi, T. L. Hughes, and S.-C. Zhang, *Phys. Rev. B* **82**, 184516 (2010).
- [44] Y. Tanaka, M. Sato, and N. Nagaosa, *J. Phys. Soc. Jpn.* **81**, 011013 (2012).
- [45] X.-P. Liu, Y. Zhou, Y.-F. Wang, and C.-D. Gong, *New J. Phys.* **19**, 093018 (2017).
- [46] T. Fukui, Y. Hatsugai, and H. Suzuki, *J. Phys. Soc. Jpn.* **74**, 1674 (2005).